Tilorone-induced lysosomal storage of glycosaminoglycans in cultured corneal fibroblasts: biochemical and physicochemical investigations

Jens FISCHER

Department of Pharmacology, University of Kiel, Hospitalstr. 4, D-24105 Kiel, Federal Republic of Germany

Tilorone (2,7-bis[2-(diethylamino)ethoxy]-fluoren-9-one) and several other bis-basic compounds are known to induce lysosomal glycosaminoglycan (GAG) storage. The responsible pathomechanism has not been elucidated yet. The assumption of an unspecific disturbance of lysosomal proenzyme targeting due to elevation of endosomal pH is opposed by the hypothesis of formation of a complex between tilorone and GAGs within the lysosomes, which renders GAGs indigestible to glycosidases. In cultures of bovine corneal fibroblasts the amounts of intracellular GAGs [dermatan sulphate (DS), heparan sulphate (HS) and chondroitin sulphate (CS)] were quantified. The fibroblasts were exposed to tilorone (5 μM), which was found to be readily taken up by the cells and to be accumulated within acidic compartments to finally achieve millimolar concentrations. Under these conditions the GAG storage is predominantly due to the accumulation of DS; however, the DS secretion into the culture medium was not affected. The HS accumulation was much less pronounced, accounting only for 3% of total GAG storage. Ammonium chloride (10 mM), which is known to diminish lysosomal enzyme activity by interfering with the mannose 6-phosphate receptor-mediated transport, prevents both HS and DS breakdown. By means of NMR spectroscopy it was shown that tilorone itself tends to display a concentration-dependent aggregation which was enhanced in the presence of GAGs. The diethylamino groups of tilorone interact physicochemically with DS, and to a smaller extent with HS, but not with chondroitin 4-sulphate. Thus, the strength of the interaction between tilorone and the different GAGs *in vitro* correlates with the potency of tilorone to inhibit the breakdown of the individual GAGs in cultured bovine fibroblasts. The results support the hypothesis of a specific interaction between tilorone and particular GAGs, rendering these resistant to enzymic degradation.

INTRODUCTION

Tilorone exhibits anti-viral and anti-tumour activities due to immunomodulatory properties [1]. The molecule (Figure 1) is characterized by a bis-basic (pK_a = 8.64, 9.27) tricyclic structure [2]. Upon chronic administration to rats, tilorone induces generalized lysosomal storage of sulphated glycosaminoglycans (GAGs) [3]. This side-effect was reproduced in cultured fibroblasts of several species [4,5]. By analogy with the inherited storage diseases, this side-effect is called drug-induced mucopolysaccharidosis. The molecular pathomechanism of this storage phenomenon is still under discussion. Among the proposals are the diminution of lysosomal enzyme contents due to interference with the mannose 6-phosphate receptor-mediated proenzyme targeting [6], and the formation of indigestible complexes between GAGs and tilorone within the lysosomes [7,8]. In addition to mucopolysaccharidosis, tilorone causes storage of polar lipids [3,9].

The purpose of the present study was: (a) to characterize the tilorone-induced GAG storage in cultured bovine fibroblasts, which have previously been shown to be a suitable model to reproduce the drug-induced mucopolysaccharidosis *in vitro* [5]; and (b) to examine the physicochemical interactions between tilorone and the GAGs which occur physiologically in those fibroblasts. The pattern of stored GAGs was analysed after treatment with tilorone and compared with that induced by NH_4Cl (10 mM). We chose ammonia for comparison, because it is known to be a weak lysosomotropic base which causes secretion of lysosomal enzymes by interference with the pH-dependent dissociation of enzyme precursors from mannose 6-phosphate receptors in the endosomes [10,11]. If tilorone rendered GAGs indigestible to lysosomal glycosidases by complex formation, it should be possible to verify this interaction by use of NMR spectroscopy. Therefore experiments were performed at tilorone concentrations which are likely to be reached within the lysosomes. Our interest was focused on tilorone for two reasons. (a) Tilorone is representative of a series of drugs which induce mucopolysaccharidosis; a better understanding of the pathomechanism may help to avoid the side-effect of this drug in future drug development. (b) Tilorone may be useful as a specific tool to inhibit GAG catabolism.

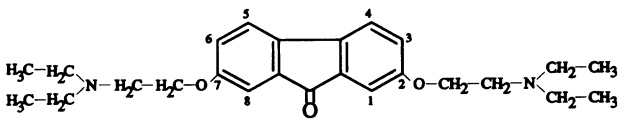

Figure 1 Chemical structure of tilorone

EXPERIMENTAL

Materials

Tilorone was kindly provided by the Merrell Dow Research Institute (Cincinnati, OH, U.S.A.). The following materials were purchased from the suppliers indicated: media and solutions for cell culture from Biochrom (Berlin, Germany) and Boehringer (Mannheim, Germany); plastic culture flasks from Falcon (Becton-Dickinson, Heidelberg, Germany); DEAE-Trisacryl M IBF and Spectra/Por membranes (1000 Da cut-off) from Serva (Heidelberg); cellulose acetate membranes and Noveco clearing solution from Bender & Hobein (Moers, Germany); SEP-PAK

Abbreviations used: GAGs, glycosaminoglycans; CS, chondroitin sulphate; C4S, chondroitin 4-sulphate; DS, dermatan sulphate; HS, heparan sulphate; MEM, minimal essential medium.

VAC/3cc C_{18} cartridges from Waters (Milford, U.S.A.); $Na_2{}^{35}SO_4$ (specific radioactivity 50–80 μCi/mmol) from Amersham-Buchler (Braunschweig, Germany); NH_4Cl, bis[2-hydroxyethyl]imino-tris[hydroxymethyl]methane (bis-tris), dermatan sulphate (DS; bovine mucosa), chondroitin 4-sulphate (C4S; bovine trachea), heparan sulphate (HS; bovine kidney), chondroitin ABC lyase (*Proteus vulgaris*, EC 4.2.2.4), chondroitin AC lyase II (*Arthrobacter aurescens*, EC 4.2.2.5) and heparin lyase III (*Flavobacterium heparinum*, EC 4.2.2.8) from Sigma (München, Germany); and Alcian Blue 8 GS from Fluka (Buchs, Swizerland). The other chemicals were of analytical grade and available from Merck (Darmstadt, Germany) and Sigma (München, Germany).

Cell culture

The bovine corneal fibroblasts were obtained by the technique described previously [5]. The cells were grown in Eagle's minimal essential medium (MEM) with Earle's salts supplemented with 10% (v/v) fetal-calf serum, non-essential amino acids and penicillin/streptomycin (100 IU/100 μg per ml) at 37 °C and 5% CO_2. The split ratio for confluent monolayers was 1:3. In this study fibroblasts from passages 4–8 were used. In some experiments GAGs of untreated fibroblasts were metabolically labelled with $^{35}SO_4{}^{2-}$. For this purpose the fibroblasts were kept for 96 h in a modified MEM which contained $MgCl_2$ instead of $MgSO_4$ and $^{35}SO_4{}^{2-}$ (1 μCi/ml).

Drug treatment

The fibroblasts were seeded into 75-cm^2 or 25-cm^2 plastic flasks. When monolayers had reached confluency the experiments were started by supplying fresh medium containing the drugs. The exposure lasted 96 h, without medium change during this period. The ratio of medium volume per culture surface was kept constant at 0.37 ml/cm^2 in all experiments. Cultures maintained simultaneously without addition of drugs served as controls.

Determination of tilorone concentrations in the culture medium

An experimental set up, previously used by MacIntyre and Cutler [12] for determination of intracellular and intralysosomal chloroquine accumulation of isolated hepatocytes, was employed to estimate the amount of tilorone taken up by the fibroblasts. The tilorone concentrations in the culture medium were determined at indicated times during the incubation period, each original value was obtained from the medium of a single culture flask (25 cm^2) which was one of several identically processed cultures. In order to analyse the tilorone content of the culture medium after incubation with non-viable cells, confluent monolayers of fibroblasts were subjected to three freeze–thaw cycles, incubated with the culture medium for 24 h and then centrifuged at 115500 *g* for 20 min. The supernatant was analysed as described below. For the purpose of estimating the proportion of intralysosomally accumulated tilorone, the intralysosomal proton concentration was lowered by means of NH_4Cl (10 mM) added 2 h prior to tilorone and present until the end (24 h) of the incubation period [12].

Tilorone was extracted by reversed-phase chromatography. Samples (5 ml) of culture medium were mixed with 5 ml ammonium sulphate buffer (0.5 M, pH 9.3) and applied to a C_{18}-column (SEP-PAK VAC/3cc C_{18}). Tilorone was retained and interfering compounds were eluted by consecutive washing with 5 ml of 0.5 M ammonium sulphate buffer (pH 9.3), 5 ml of 0.05 M ammonium sulphate buffer and 20 ml of 0.05 mM ammonium sulphate buffer (pH 9.3) containing 10% (v/v) acetonitrile. Finally, tilorone was eluted by application of 3 ml of 0.07 M phosphate buffer (pH 2.1) containing 30% (v/v) acetonitrile. The tilorone concentration was determined photometrically at 270 nm. Recoveries were 90±5% (±S.E.M., $n = 6$).

Isolation of GAGs

The GAGs were isolated from three compartments. The GAGs from the extracellular compartment, which contains exocytosed proteoglycans, were obtained from the culture medium [13]. After removal of the medium, cells were washed with PBS and harvested by trypsinization [0.1% (w/v), 10 min, 37 °C]. Cells were centrifuged and the pericellular GAGs were obtained from the supernatant [13]. Prior to isolation of intracellular GAGs the fibroblasts were homogenized.

GAGs from the three compartments were isolated in the same manner. In the first step protein cores and residual amino acids were removed by a β-elimination reaction (0.1 M NaOH final concentration, 24 h, 38 °C) in the presence of 1 M sodium borohydride. Acetic acid (20%, v/v) was added in order to neutralize the samples and 0.1% (w/v) Triton X-100 to reduce non-specific adsorption. The samples were then dialysed (Spectra/Por 6, molecular mass cut-off 1000 Da) at 4 °C for 2 days against two changes of deionized water, followed by dialysis at 4 °C for 1 day against the buffer in which the ion-exchange chromatography was performed [50 mM bis-tris, 0.1% (w/v) Triton X-100, pH 6]. Each sample was applied to a column (0.8 cm × 1 cm) of DEAE-Trisacryl M IBF. Unbound molecules were washed through the column with 5 ml of the bis-tris buffer, then 5 ml of the bis-tris buffer containing 0.3 M NaCl was applied and recovery of GAGs was finally achieved by elution with 3 ml of 1.3 M NaCl dissolved in the bis-tris buffer. After dialysis at 4 °C for 3 days against three changes of deionized water, GAGs were lyophilized and dissolved in appropriate volumes of deionized water. These concentrated GAG solutions were used for qualitative and quantitative analysis. It should be emphasized that the data, which were obtained by this method (cleavage of the protein–carbohydrate linkage region by β-elimination), did not allow conclusions as to whether the indicated GAGs originated from intact proteoglycans or had existed as free GAG chains in the culture system. Under this premise the abbreviation GAG is used throughout the text.

Electrophoresis and densitometric scanning

Electrophoretic separation of GAGs with respect to the different carbohydrate backbones was achieved at room temperature on cellulose acetate membranes (60 mm × 150 mm) in 0.1 M barium acetate solution at a constant potential of 100 V for 3.5 h [14]. The membranes were stained with an Alcian Blue solution (0.5 g Alcian Blue dissolved in 100 ml methanol/100 ml deionized water/10 μl acetic acid) for 10 min and destained with three changes of 0.83 mM acetic acid within 10 min [8]. To fix the cellulose acetate strips on microscope slides, Noveco clearing solution was used. A mixture of C4S, DS and HS in aqueous solution served as a reference. In parallel with the Alcian Blue stain, radioactively labelled GAG bands were visualized by autoradiography on an X-ray film (Kodak X-Omat MA).

The quantitative analysis of the GAG pattern was accomplished by densitometric scanning of Alcian Blue-stained strips [15,16]. The densitometric scans were performed at 568 nm using a CAMAG TLC II scanner. Samples were quantified by means of standard curves established by plotting known amounts of reference GAGs versus the area under the corresponding densitometric curves.

Enzymic and chemical degradation of GAGs

The GAGs were further identified by enzymic and chemical degradation reactions. Parallel digestions were performed with chondroitin ABC lyase in enriched Tris buffer [17], with chondroitin AC II lyase in enriched sodium acetate buffer [18] and with heparin lyase III in sodium acetate buffer [19]. The digestion with each of the enzymes was done with 0.05 unit of the respective enzymes in a total volume of 200 μl. The samples were incubated (37 °C), for 30 min in the case of chondroitin ABC lyase and chondroitin AC II lyase, and for 60 min in the case of heparin lyase III. The reactions were stopped by freezing for lyophilization. Controls were run by incubations of GAGs in the respective buffers without the enzymes. Additionally, HS was depolymerized by the low pH procedure of Shively and Conrad [20]. The degraded GAG samples were again applied to a DEAE-Trisacryl M IBF column (0.4 cm × 1 cm), dialysed, lyophilized and applied to electrophoresis as described above.

NMR spectra

Tilorone was dissolved in deuterated phosphate buffer (0.15 M, pH 7.0) and added to solutions of DS, HS and C4S. The volume changed only negligibly by adding increasing amounts of tilorone. The concentrations of galactosaminoglycans were calculated with reference to the average molecular masses of the disaccharide units. Acetone was used as internal standard to control field homogeneity in the interaction studies. The experiments were performed with an AM360L spectrometer (Bruker Darmstadt, Germany) at a probe temperature of 23 °C. Data acquisition included 128 scans, 16K free induction decays, sweep width of 4098 Hz, 0.25 Hz/Pt and homonuclear presaturation to depress water signals.

Reproducibility was checked by repetition of the experiments. The significance of $1/T_2$ changes can be derived from the following observations: (1) the area under the curve remains constant; and (2) the resonance signals remain symmetric.

RESULTS

GAGs of untreated bovine fibroblasts

HS and two galactosaminoglycans were isolated from the intracellular and pericellular compartments of the bovine corneal fibroblasts (Figures 2a and 2b). The autoradiography from an electrophoretic separation showed that the bands stained by Alcian Blue all contained ^{35}S, indicating that the isolated GAGs were endogenously synthesized and labelled during the incubation period. The only exception was the non-labelled chondroitin sulphate (CS) band of the extracellular compartment, which was found to originate from the fetal-calf serum (results not shown). Figure 3 depicts the electrophoretic separation of pericellular GAGs after the degradation procedures. Similar results were obtained with the intracellular and extracellular GAGs. As judged from the electrophoretic separation, the galactosaminoglycans appeared to represent DS and CS, although apparent CS was only partially degraded by chondroitin AC II lyase. This property would be characteristic for a DS/CS co-polymer, which on the one hand contains enough β-D-glucuronic acid to resemble CS on electrophoresis, but on the other hand contains sufficient amounts of α-L-iduronic acid to be prevented from complete degradation by chondroitin AC lyase II [21]. HS derived from the intracellular and pericellular compartments showed the appropriate susceptibility to the different degradation procedures (Figure 3). Table 1 indicates the relative amounts of HS and of both galactosaminoglycans isolated from

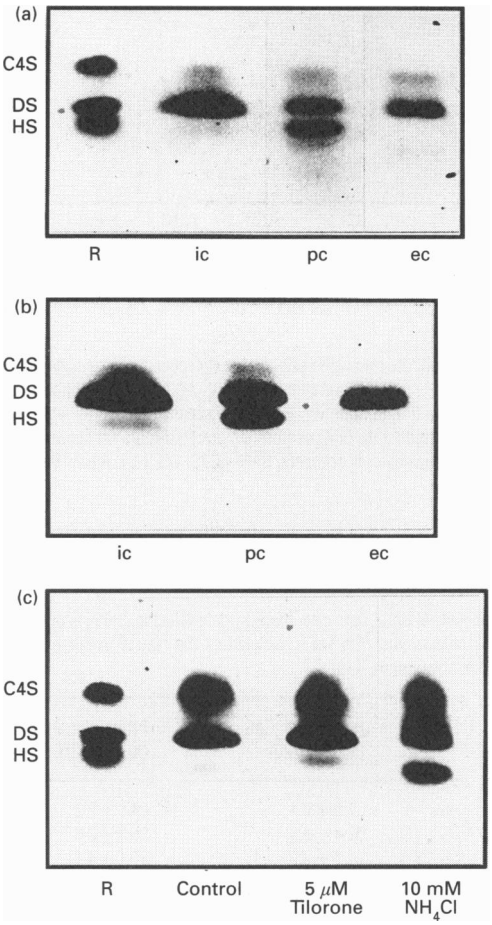

Figure 2 GAGs derived from untreated cultures of bovine corneal fibroblasts

Cellulose acetate electrophoresis of GAGs isolated from the intracellular (ic), pericellular (pc) and extracellular (ec) compartments after metabolic labelling with $^{35}SO_4^{2-}$ (1 μCi/ml, 96 h). In (**a**) bands are stained with Alcian Blue. The positions of the reference compounds C4S, DS and HS are given on the left-hand lane (R). (**b**) shows the autoradiography of the same electrophoretic strip. (**c**) Cellulose acetate electrophoresis of intracellular GAGs after treatment (96 h) of fibroblasts with 5 μM tilorone and 10 mM NH_4Cl. The left-hand lane shows the positions of reference GAGs (R). Alcian Blue stain.

the intracellular and pericellular compartments. Keratan sulphate was not detected. Although keratan sulphate is an important constituent of the corneal extracellular matrix *in vivo*, cultures of corneal fibroblasts are known to synthesize only small quantities of keratan sulphate (about 2 % of total GAGs). The present data are in accordance with previous reports by other authors [13,22]. In the extracellular compartment DS was found to be the predominant GAG.

Intracellular GAGs after drug treatment

Fibroblasts were treated with 5 μM tilorone for 96 h and in parallel with 10 mM NH_4Cl. Representative electrophoretic separations of intracellular GAGs after treatment with the indicated agents are shown in Figure 2(c). The susceptibility of GAGs from drug-treated fibroblasts towards the degradation procedures was identical to that found for pericellular GAGs and for untreated fibroblasts (results not shown). Increases of the intracellular GAG contents were expressed as multiples of the values obtained with untreated controls, which were included in

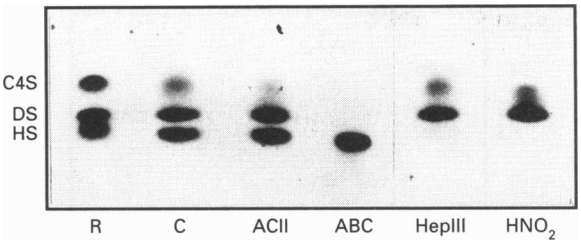

Figure 3 Degradation of pericellular GAGs by enzymic or chemical procedures

The different lanes indicate electrophoresis after treatment with control buffer of the chondroitin lyase AC II digestion (C), with chondroitin lyase AC II (ACII), with chondroitin lyase ABC (ABC), with heparin lyase III (HepIII) and with HNO_2. The separation of GAGs which were incubated with control buffers used for the other degradation procedures are not shown. The left-hand lane (R) represents the separation of reference GAGs (C4S, DS, HS). Alcian Blue stained.

Table 1 Patterns of intracellular and pericellular GAGs in cultures of untreated bovine corneal fibroblasts

The relative amounts of GAGs were determined by densitometric scanning of Alcian Blue-stained electrophoretic preparations. The Table summarizes the results (mean ± S.E.M.) from three different cell lines (passages 4–8).

	Intracellular GAG (%) ($n = 20$)	Pericellular GAG (%) ($n = 10$)
HS	7.9 ± 0.4	34.6 ± 2.2
DS	57.4 ± 3.6	35.3 ± 2.6
CS/DS	34.7 ± 3.9	30.1 ± 4.1

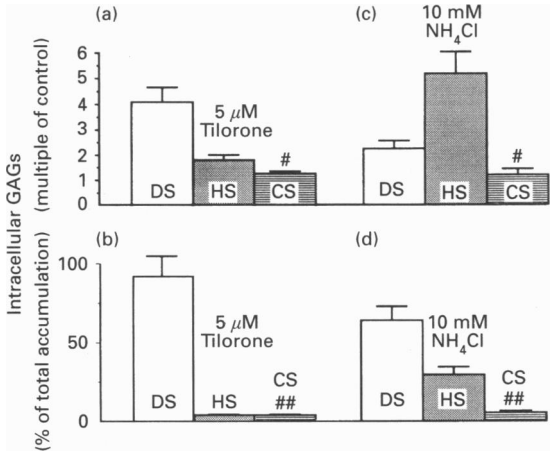

Figure 4 Quantitative analysis of intracellular GAGs after treatment (96 h) with tilorone (a, b) and NH_4Cl (c, d)

The amounts of intracellular GAGs were determined by densitometric scanning of Alcian Blue-stained bands after electrophoretic separation. In (**a** and **c**), the data are expressed as multiples of controls. In (**b** and **d**), contributions of individual GAGs towards the total intracellular GAG accumulation are shown. Bars represent data (mean ± S.E.M., $n = 6$–7) from three different cell lines; #, not significantly different from 1; ##, not significantly different from 0.

each experiment. Tilorone (5 μM, 96 h) induced an increase of DS by a factor of 4. HS was augmented only by a factor of 1.8 and CS/DS by a factor of 1.2 (Figure 4a). Looking at the

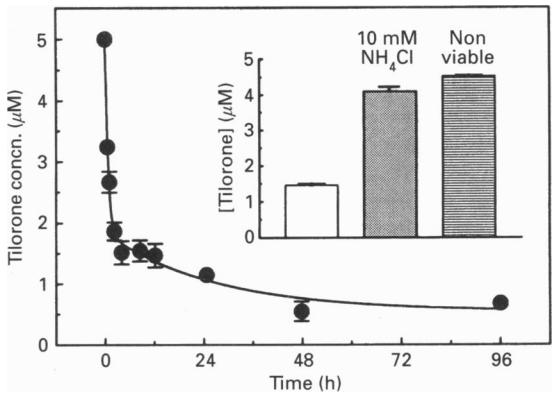

Figure 5 Time-dependent decline of tilorone concentration in the culture medium

Tilorone concentration declines bi-exponentially during an incubation period of 96 h. The inset shows the tilorone concentrations (at 24 h) under standard conditions (open column), in the presence of 10 mM NH_4Cl, and upon incubation with non-viable cells (three thaw–freeze cycles). Data are expressed as mean values (± S.E.M.) derived from 3–5 experiments.

amount of GAGs which were accumulated during the experimental period, it became evident that DS represented over 90% of the accumulated GAGs (Figure 4b).

The pattern of intracellular GAGs after treatment with NH_4Cl was different from that after exposure to tilorone (Figure 4c): DS was increased by a factor of 2.2 only, whereas HS was augmented 5-fold. As a consequence, the contribution of HS to the total intracellular GAG storage (Figure 4d) was increased, namely 30% as opposed to 3% in the case of tilorone-treated cells.

Extracellular and pericellular DS

Theoretically, an impaired secretion of proteoglycans, rather than the disturbance of lysosomal degradation, could be responsible for increased intracellular GAG contents. Since the tilorone-induced GAG storage consisted of an almost selective DS accumulation, it was examined whether the amount of secreted DS was altered after treatment for 96 h with tilorone. For this purpose culture media of tilorone-treated cells and untreated fibroblasts were analysed for DS contents. The amount of extracellular DS was found to be unchanged in the presence of tilorone (100 ± 23% of controls; mean ± S.E.M.; $n = 4$), indicating normal secretion of DS. The pericellular DS was also analysed. In cells treated with 5 μM tilorone, it amounted to 140 ± 29% (± S.E.M.; $n = 3$) of the control values. The difference was not statistically significant.

Estimation of intralysosomal tilorone concentration

The time course of the tilorone uptake by fibroblasts was monitored indirectly by following the decline of drug concentration in the culture medium [12]. The initial medium concentration of 5 μM declined to values below 1 μM during the incubation period (Figure 5). The bi-exponential decay was characterized by $t_{\frac{1}{2}}$ values of 30 min and 19 h. After incubation of non-viable fibroblasts for 24 h the concentration fell to 4.5 μM only, instead of 1.5 μM in the case of viable cells. These results demonstrated that viability of cells was a prerequisite for the tilorone uptake and showed that physicochemical drug binding to pericellular GAGs and phospholipid membranes, drug intercalation into DNA, or unspecific adsorption to the culture-dish surfaces did not make major contributions to the dis-

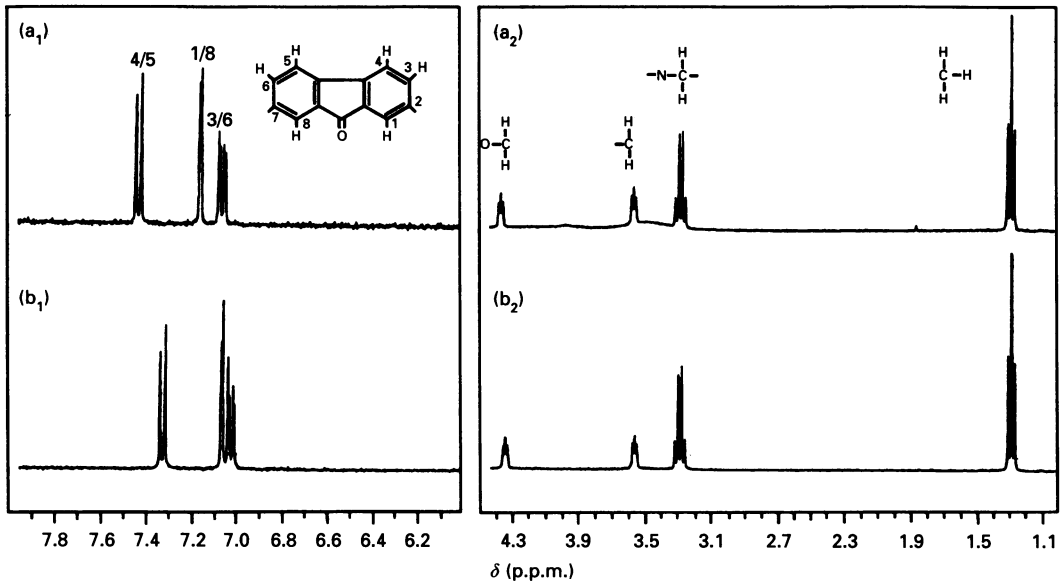

Figure 6 NMR proton resonance signals of tilorone in aqueous solution (0.15 M phosphate buffer, pH 7)

The spectrum of tilorone at 0.2 mM is depicted in ($\mathbf{a_1}$) and ($\mathbf{a_2}$). The spectrum of tilorone at 2.0 mM is shown in ($\mathbf{b_1}$) and ($\mathbf{b_2}$). As compared with ($\mathbf{a_{1/2}}$) at 2.0 mM the aromatic proton signals shifted to higher fields ($\mathbf{b_1}$). The proton signals of the ether structure shifted upfield, too ($\mathbf{b_2}$), but to a less pronounced degree, whereas the aliphatic proton signals of the diethylamino-group moved slightly downfield.

appearance of tilorone from the medium. In the presence of NH_4Cl the medium concentration of tilorone fell to 4.1 μM only, indicating that the decline of tilorone concentration was, for the most part, a consequence of drug trapping in the acidic cellular compartments.

From the difference between the amounts of tilorone disappearing from the medium within 24 h in the absence and in the presence of NH_4Cl it could be calculated that at least 1 nmol of tilorone/cm^2 cell layer was trapped in acidic compartments. The width of the cell layer was approx. 2 μm, as estimated on microscopic cuts peripendicular to the culture surface (R. Lüllmann-Rauch, personal communication). For a confluent cell layer, the total cellular volume could be calculated to be 0.2 μl/cm^2 of culture surface. This yielded an intracellular tilorone concentration of 5 mM. The lysosomal volume of normal fibroblasts has been reported to occupy 3–4% of the total cellular volume [23,24]. Taking into account the enlargement of the lysosomes after treatment with tilorone, the volume of lysosomes might occupy 10% of cellular volume [25]. Thus, the intralysosomal concentration of tilorone can be estimated to amount to approx. 50 mM at 24 h after the start of exposure to an initial medium concentration of 5 μM. These calculations were based on cautious assumptions, since ammonia probably did not completely abolish the trapping of tilorone, and since the tilorone uptake was not in equilibrium after 24 h. Even if we overestimated the amount of tilorone which reached the lysosomal compartment, there is no doubt that the lysosomal tilorone concentration was in the millimolar range.

NMR spectra

Intermolecular interaction of tilorone

An attempt to answer the question of whether tilorone is able to interact with the GAG species physiologically occurring in cultures of bovine corneal fibroblasts was made using NMR spectroscopy of tilorone and tilorone/GAG mixtures.

First, NMR spectra of pure aqueous tilorone solutions were recorded. An increase of the drug concentration from 0.2 mM to 2 mM led to a strong shift of aromatic proton signals to higher fields (Figure 6). This shift of aromatic proton signals was linearly correlated with the increase of tilorone concentration. In Figure 7(a) this is shown for the protons 4/5 of the fluorenone nucleus. The proton signals derived from the methylene groups of the ether structure (Figure 7b) shifted upfield too, although less than the aromatic proton signals, whereas the resonance signals of the diethylamino structure were hardly influenced at all (Figures 7c and 7d). Thus, the changes in chemical shifts of proton signals decreased as a function of the distance from the aromatic fluorenone nucleus. In the concentration range investigated, no broadening of proton signals occurred. The strong shift of aromatic proton signals indicated intermolecular associations of the aromatic fluorenone nuclei, which led to the formation of charge-transfer complexes in aqueous solutions.

Influence of GAGs on the aromatic proton signals of tilorone

C4S failed to induce an additional shift of the aromatic proton signals (Figure 7, II), although the signals displayed a moderate broadening in the presence of C4S, which was not observed in pure tilorone solutions (Figure 8b). In the presence of HS (6.36 mM) the NMR spectrum of tilorone (1.818 mM) showed a strong shift of the aromatic proton signals to higher fields (Figure 7, II). Additionally the signals were broadened (Figure 8c) to a greater extent than those obtained with the C4S/tilorone combination (Figure 8b). This change in $1/T_2$ can be related to a decrease in rotational freedoms. In the presence of DS, the chemical shift of aromatic proton signals was equal to that seen with HS (Figure 7, II). With respect to broadening of the signals, DS exhibited the strongest effect (Figure 8d). Thus, DS showed the strongest interaction with tilorone, whereas C4S showed the weakest.

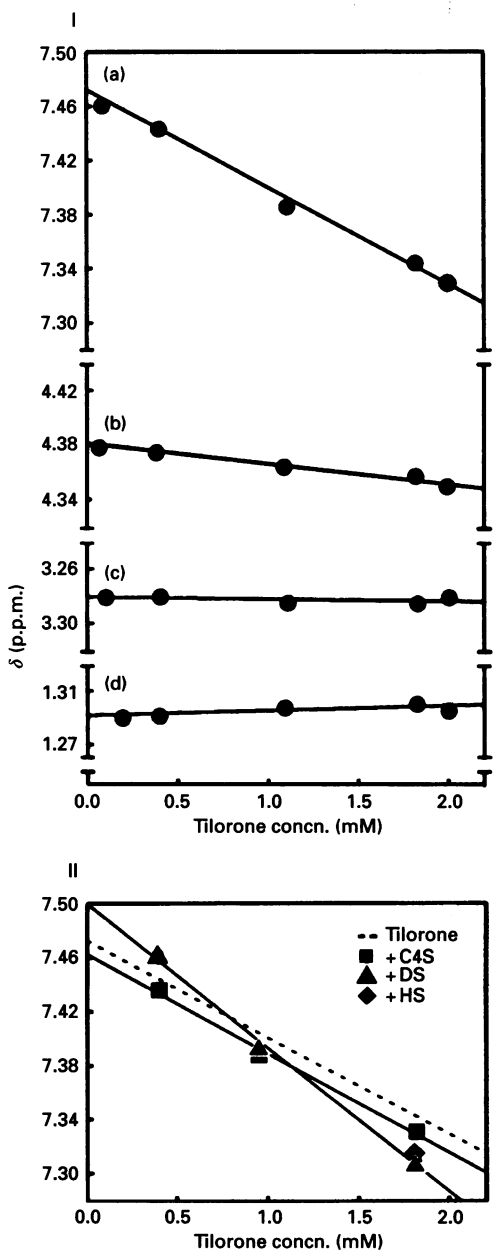

Figure 7 Concentration-dependent changes in chemical shifts of tilorone protons

(I) (**a**) Aromatic protons at position 4/5 of the fluorenone nucleus; (**b**) methoxy group; (**c**) methylene group of the diethylamino structure; (**d**) methyl group. This Figure shows that the shift of proton resonances declines as a function of distance from the aromatic nucleus, indicating intermolecular association of aromatic ring systems. (II) Influence of C4S, DS and HS on the chemical shifts of aromatic protons at position 4/5 of the tilorone nucleus. The broken line represents the data of aqueous tilorone solutions without addition of GAGs, which have also been included in (**a**). C4S was present at 6.07 mM, DS at 6.36 mM and HS at 6.36 mM. In case of HS, NMR spectrometry was performed at a single tilorone concentration of 1.818 mM. At 1.818 mM tilorone the chemical shift of protons was nearly identical in the presence of DS and HS. DS and HS enhanced the shift of the aromatic proton resonance to higher fields.

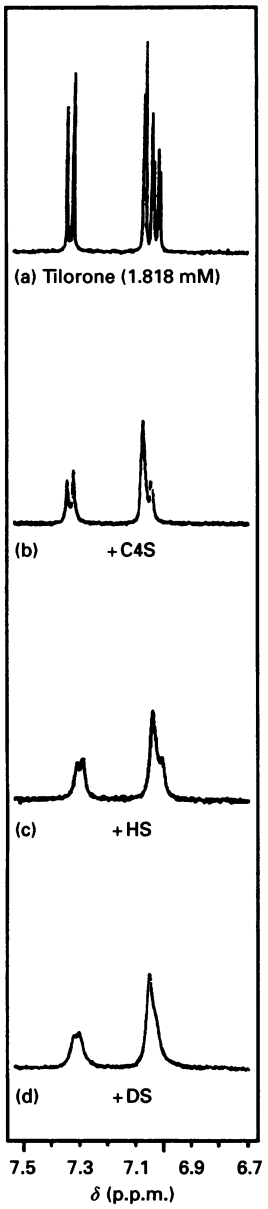

Figure 8 Parts of NMR spectra showing the resonance signals of aromatic tilorone protons

(**a**) Spectrum represents a tilorone solution in phosphate buffer (pH 7) at a drug concentration of 1.818 mM. The spectrum in the presence of C4S (6.07 mM) is depicted in (**b**), of HS (6.36 mM) in (**c**), and of DS (6.36 mM) in (**d**). DS induced the strongest signal broadening of aromatic proton signals.

Influence of GAGs on the aliphatic proton signals of tilorone

If the assumption of an electrostatic interaction between protonized diethylamino groups of tilorone and polyanionic GAGs is correct, the aliphatic proton signals of diethylamino groups should also be broadened because of diminished rotational freedom. In the presence of CS (Figure 9b) the resonance signals of diethylamino protons remained unchanged. Only the methylene protons of the ethoxy structure showed slight broadening of signals. The effects of HS (6.36 mM) are depicted in Figure 9(c). It is obvious that HS caused distinct broadening of diethylamino proton signals and also of ethoxy proton signals. DS induced the strongest broadening of the aliphatic proton signals (Figure 9d). This DS-induced broadening increased with rising tilorone concentrations (results not shown), indicating that the strength of interaction was positively correlated with increased tilorone/DS ratios.

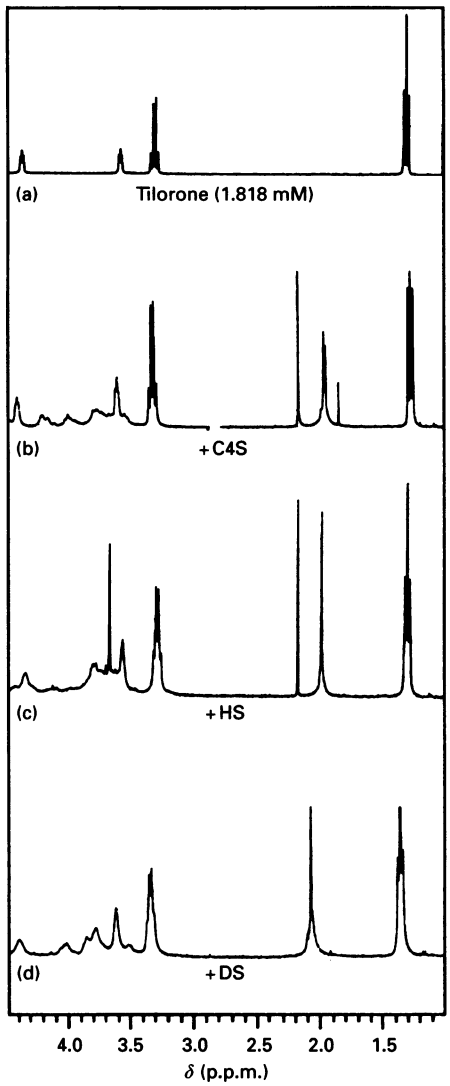

Figure 9 Parts of NMR spectra showing the resonance signals of aliphatic tilorone protons

(**a**) Spectrum is derived from a solution (phosphate buffer, pH 7) containing tilorone at a drug concentration of 1.818 mM. The spectra after addition of C4S (6.07 mM), of HS (6.36 mM) and of DS (6.36 mM) are shown in (**b**), (**c**) and (**d**). The signal broadening of diethylamino protons indicate an interaction of this group with the GAGs, DS induced the strongest effect, C4S the weakest.

DISCUSSION

In the first part of the present study it was demonstrated that the exposure (96 h) of bovine corneal fibroblasts to tilorone (5 μM) results in a predominant storage of DS, which amounts to about 90% of total GAG storage. Thus, the DS accumulation can be taken as the biochemical correlate of the histochemical and ultrastructural alterations in the bovine fibroblast lysosomes observed after treatment with 5 μM tilorone [5]. The observation that after application of NH_4Cl the DS storage was less, while the HS storage was more pronounced, emphasized the selectivity of tilorone-induced DS storage. In the case of NH_4Cl it is well known that the rather unspecific disturbance of the digestive function of lysosomes [10] is due to increased endosomal and lysosomal pH values [26,27] which results (a) in diverting lysosomal proenzymes into the culture medium, and (b) in deviation from the pH optimum of GAG-degrading enzymes. It has been shown under experimental conditions identical to those of the present study, that NH_4Cl (10 mM) indeed induced secretion of lysosomal enzymes, whereas tilorone (5 μM) did not [28,29]. Theoretically, tilorone could inhibit GAG-catabolizing enzymes either (a) directly or (b) indirectly by elevating the lysosomal pH. Since DS was accumulated to a greater extent than HS, the inhibitory effect of tilorone should be more pronounced upon DS-catabolizing enzymes. It has been demonstrated in biochemical enzyme assays [6] that tilorone up to 100 μM does not inhibit any of the exoglycosidases and exosulphatases involved in GAG degradation. Despite this finding a direct inhibition cannot be excluded, since the present data of the tilorone uptake show that during incubation with an initial concentration of 5 μM, the intralysosomal drug concentration reaches the millimolar range. The indirect inhibition of enzymic activity in the lysosomes due to increased pH could arise as well on a prelysosomal as on a lysosomal level. The prelysosomal disturbance of mannose 6-phosphate receptor-mediated proenzyme targeting is not restricted to particular enzymes, as far as soluble enzymes are concerned. Thus, this mechanism is not capable of explaining the predominant DS storage after treatment with 5 μM tilorone. The elevation of lysosomal pH could be responsible for diminished enzyme activity, if the pH raises to values inappropriate for the action of the glycosidases. Again it would be difficult to explain why treatment with tilorone should affect DS metabolism to a greater extent than HS metabolism, since different susceptibility of the DS- and HS-catabolizing enzymes towards pH changes has not been reported. Finally, the marked storage of both DS and HS after treatment with NH_4Cl clearly shows that the elevation of prelysosomal and lysosomal pH does not result in specific DS storage.

Alternatively, the increased intracellular GAG content could be caused either by an increased synthesis or by impaired secretion. An enhanced synthesis seems to be rather improbable, since, at least in human fibroblasts, 10 μM tilorone did not affect cellular GAG synthesis [6]. Impaired secretion can be excluded by the finding of an unaltered extracellular DS content in the present study.

Another mechanism which has been proposed for drug-induced mucopolysaccharidosis [7,8] resembles the mechanism of drug-induced lipidosis [30], assuming the formation of complexes between substrate and drug which resist enzymic degradation. It is obvious that GAGs are able to form complexes with cationic molecules. This property leads, for instance, to selective staining of GAGs with cationic dyes in the presence of high Mg^{2+} concentrations [31], or to the isolation of GAGs by means of anionic-exchange chromatography. Thus, even in the case of polyanionic DS and di-cationic tilorone molecules, electrostatic forces should initiate the formation of complexes within the lysosomes. In the present study this complex formation was verified by recording NMR spectra of aqueous solutions containing both tilorone and DS at concentrations which are reached in the lysosomes of cultured fibroblasts. A strong interaction between DS and tilorone was proved by shifts and broadening of aromatic and aliphatic proton signals of tilorone in the presence of the galactosaminoglycan. The data obtained with solutions containing tilorone alone suggest that the fluorenone nuclei of tilorone molecules form charge-transfer complexes at millimolar concentrations. DS enhanced the changes in the chemical shifts of aromatic proton signals of tilorone and induced, in addition, signal broadening, indicating an interaction between DS and charge-transfer complexes of tilorone. The additional shift and the signal broadening suggest a closer approximation of tilorone molecules within the charge-transfer complexes due to the

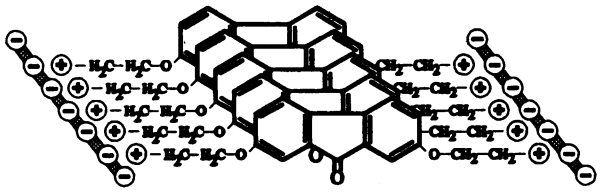

Figure 10 Model of the tilorone–GAG interaction

The spectroscopic data suggested a simultaneous interaction (a) between protonized diethylamino groups (symbolized as ⊕) of tilorone and polyanionic GAGs and (b) between π-electrons of adjacent fluorenone ring systems. The depicted model allows these interactions by assuming a parallel array of tilorone molecules, which were associated to multimeric complexes and bridge between at least two GAG chains.

presence of the carbohydrate backbone. The finding that the fluorenone nuclei aggregate even in the presence of DS was astonishing, because the ratios of anionic binding sites (at least two per disaccharide unit) and tilorone molecules ranged from about 60:1 (0.2 mM tilorone) to about 7:1 (1.818 mM tilorone). Assuming random distribution of tilorone molecules over the entire carbohydrate backbone, the emerging distances would be too long for an intermolecular interaction between adjacent fluorenone nuclei. The present data are consistent with the hypothesis that clusters of tilorone charge-transfer complexes bridge between at least two DS chains (Figure 10). This model allows the close approximation of fluorenone nuclei in a parallel array, while the protonized nitrogens associate with anionic carboxyl and sulphate groups. The present findings are in line with data from thermodynamic binding studies concerning the DS/Acridine Orange system [32]. Those data indicate that DS binds about two molecules of Acridine Orange per disaccharide unit, suggesting that sulphate and carboxylate groups serve as binding sites. Similar to the present findings with tilorone, the nuclei of Acridine Orange were shown to display a strong intermolecular interaction on the backbone of DS. Taking into account the intracellular amounts of tilorone and of DS (results not shown) the molar ratio comes up to 3:1 in cultured fibroblasts. Since tilorone is assumed to form complexes also with polar lipids within the lysosomes [30] the ratio between tilorone and disaccharides may be less than 3:1. These calculations are in accordance with results from animal experiments which suggest that 1–2 molecules of tilorone bind to one disaccharide unit of DS [8]. Although NMR data of DS were not available in this study, the stoichiometric considerations support the hypothesis that carboxylate and sulphate groups of DS are the binding sites for the di-cationic tilorone molecules in lysosomes of living cells also. The NMR spectra of tilorone/HS mixtures showed that the interaction between the cationic amino groups and HS was qualitatively the same, but weaker as compared with the DS/tilorone interaction. No interaction was observed between the tilorone side chains and CS.

DS, CS and HS display helical secondary conformations in aqueous solutions. Their primary structures differ with respect to the amino sugars, the positions and abundance of sulphate groups and the degree of uronic acid epimerization. Their secondary conformations differ with respect to the ring conformation of uronic acids, the distance of sulphate groups to the centre line of the carbohydrate chains and the distances between negative charges. These differences, in combination with those concerning the orientation and size of hydrophobic domains, the charge density and extent of intramolecular hydrogen-bonding, are thought to determine the ability of certain GAGs to interact with environmental structures [33–36]. It is conceivable that these conformational differences between HS, DS and CS account also for the different strength of interactions with tilorone. The degree of interactions between tilorone and different GAGs *in vitro* correlated well with the GAG storage induced by tilorone in cultured fibroblasts, supporting the proposed causal relationship. Further investigations are necessary to prove whether tilorone–DS complexes are indeed indigestible for lysosomal glycosidases and whether the GAG storage is due to impaired degradation of proteoglycans or free GAG chains.

I gratefully acknowledge recording of the NMR-spectra by Ing. grad. H. P. Cordes and the helpful discussion of the NMR-spectra with Professor J. K. Seydel (Institute of Experimental Biology and Medicine, D-23845, Borstel).

REFERENCES

1 Regelson, W. (1981) Pharmacol. Therap. **15**, 1–44
2 Chandra, P. and Wright, G. J. (1977) Top. Curr. Chem. **72**, 125–148
3 Hein, L. and Lüllmann-Rauch, R. (1989) Toxicology **58**, 145–154
4 Burmester, J., Handrock, K. and Lüllmann-Rauch, R. (1990) Arch. Toxicol. **64**, 291–298
5 Lüllmann-Rauch, R. and Ziegenhagen, M. (1991) Virchows Arch. (Zellpathol.) **60**, 99–104
6 Gupta, D. K., Gieselmann, V., Hasilik, A. and Von Figura, K. (1984) Hoppe Seyler's Z. Physiol. Chem. **365**, 859–866
7 Grave, S., Lüllmann, H., Lüllmann-Rauch, R., Osterkamp, G. and Prokopek, M. (1992) Toxicol. Appl. Pharmacol. **114**, 215–224
8 Prokopek, M. (1991) Biochem. Pharmacol. **42**, 2187–2191
9 Lüllmann-Rauch, R. (1983) Virchows Arch. (Zellpathol.) **44**, 355–368
10 Seglen, P. O. (1983) Methods Emzymol. **96**, 737–764
11 Gonzalez-Noriega, A., Grubb, J. H., Talkad, V. and Sly, W. S. (1980) J. Cell Biol. **85**, 839–853
12 MacIntyre, A. C. and Cutler, D. J. (1988) J. Pharm. Sci. **77**, 196–199
13 Bleckmann, H. and Kresse, H. (1980) Exp. Eye Res. **30**, 469–479
14 Wessler, E. (1968) Anal. Biochem. **26**, 439–444
15 Curwen, K. D. and Smith, S. C. (1977) Anal. Biochem. **79**, 291–301
16 Stramm, L. E., Li, W., Aguirre, G. D. and Rockey, J. (1987) Exp. Eye Res. **44**, 17–28
17 Saito, H., Yamagata, T. and Suzuki, S. (1968) J. Biol. Chem. **243**, 1536–1542
18 Hiyama, K. and Okada, S. (1975) J. Biol. Chem. **250**, 1824–1828
19 Linker, A. and Hovingh, P. (1965) J. Biol. Chem. **240**, 3724–3728
20 Shively, J. E. and Conrad, H. E. (1976) Biochemistry **15**, 3932–3942
21 Habuchi, H., Yamagata, T., Iwata, H. and Suzuki, S. (1973) J. Biol. Chem. **248**, 6019–6028
22 Bleckmann, H. and Kresse, H. (1979) Graefes Arch. Clin. Exp. Opthal. **210**, 291–300
23 Hollemanns, M., Elferink, R. O., De Groot, P. G., Strijland, A. and Tager, J. M. (1981) Biochim. Biophys. Acta **643**, 140–151
24 De Duve, C., De Barsy, T., Poole, B., Trouet, A., Tulkens, P. and Van Hoof, F. (1974) Biochem. Pharmacol. **23**, 2495–2531
25 Wibo, M. and Poole, B. (1974) J. Cell Biol. **63**, 430–440
26 Ohukuma, S. and Poole, B. (1978) Proc. Natl. Acad. Sci. U.S.A. **75**, 3327–3331
27 Polle, B. and Ohukuma, S. (1981) J. Cell Biol. **90**, 665–669
28 Lüllmann-Rauch, R., Pods, R. and Von Witzendorff, B. (1995) Biochem. Pharmacol. **49**, 1223–1233
29 Lüllmann-Rauch, R. and Ziegenhagen, M. (1993) Naunyn Schmiedebergs Arch. Pharmacol. **347**, R110
30 Lüllmann, H., Lüllmann-Rauch, R. and Wassermann, O. (1978) Biochem. Pharmacol. **27**, 1103–1108
31 Scott, J. E. (1980) Biochem. J. **187**, 887–891
32 Menter, J. M., Hurst, R. E. and West, S. S. (1977) Biopolymers **16**, 695–702
33 Scott, J. E., Chen, Y. and Brass, A. (1992) Eur. J. Biochem. **209**, 675–680
34 Scott, J. E. (1992) FASEB J. **6**, 2639–2645
35 Scott, J. E. and Heatley, F. (1982) Biochem. J. **207**, 139–144
36 Scott, J. E., Heatley, F., Jones, M. N., Wilkinson, A. and Olavesen, A. H. (1983) Eur. J. Biochem. **130**, 491–495

Received 25 April 1995/7 July 1995; accepted 27 July 1995